arXiv:cond-mat/0306423v2 [cond-mat.mes-hall] 23 Jun 2003

Dynamics of disordered quantum Hall crystals

Michael M. Fogler

University of California San Diego, Department of Physics, 9500 Gilman Drive, La Jolla, CA 92093-0319, USA

Abstract

Charge density waves are thought to be common in two-dimensional electron systems in quantizing magnetic fields. Such phases are formed by the quasiparticles of the topmost occupied Landau level when it is partially filled. One class of charge density wave phases can be described as electron solids. In weak magnetic fields (at high Landau levels) solids with many particles per unit cell - bubble phases - predominate. In strong magnetic fields (at the lowest Landau level) only crystals with one particle per unit cell - Wigner crystals - can form. Experimental identification of these phases is facilitated by the fact that even a weak disorder influences their dc and ac magnetotransport in a very specific way. In the ac domain, a range of frequencies appears where the electromagnetic response is dominated by magnetophonon collective modes. The effect of disorder is to localize the collective modes and to create an inhomogeneously broadened absorption line, the pinning mode. In recent microwave experiments pinning modes have been discovered both at the lowest and at high Landau levels. We present the theory of the pinning mode for a classical two-dimensional electron crystal collectively pinned by weak impurities. We show that long-range Coulomb interaction causes a dramatic line narrowing, in qualitative agreement with the experiments.

Key words: pinning, Wigner crystal, charge-density wave, two-dimensional electron gas, magnetophonon
PACS: 74.40.Xy, 71.63.Hk

1. Introduction

Two-dimensional electron gas (2DEG) in quantizing magnetic fields is known to be a system with a rich phase structure. Recently, much attention has been devoted to charge-density wave phases, which include stripe phase, bubble phase, and a Wigner crystal [1,2,3]. An important new information on the dynamics of such phases was provided by a group of microwave experiments [4,5,6,7,8]. They demonstrated that the low-frequency ac response of magnetic-field-induced charge-density waves is strongly affected by disorder, in ways not anticipated in prior theoretical work on the subject. Motivated by these intriguing results, Huse and the present author [9] reconsidered the problem of collective dynamics of a Wigner crystal pinned by quenched disorder. Here I give a brief account of this work and its more recent extensions. Much of the foregoing discussion also applies to the bubble phase. The rest of this section is devoted to a brief introduction to the charge-density wave phases, conventional expectations regarding the response of a pinned system, and how they compare with the observed behavior. Sections 2 and 3 outline our theoretical model and its analysis. Finally, Sec. 4 contains comparison of our theory with the experiment and concluding remarks.

The bubble phase [3] can be viewed as a crystal made of multi-electron droplets (bubbles). The number of particles per bubble M depends on the Landau level

filling fraction ν and changes in discrete steps at certain critical values of ν. Here M counts only the quasiparticles of the topmost (Nth) Landau level, which is partially filled. The other Landau levels are completely filled and in a first approximation, provide an inert background of constant uniform density. Bubble phases with $M > 1$ appear when three or more Landau levels are populated, $\nu > 4$ ($N \geq 2$). The Wigner crystal is the $M = 1$ bubble phase (one particle per unit cell). It forms at any Landau level N provided ν is close enough to an integer. We refer to the bubble and the Wigner crystal phases jointly as electron crystals. At zero temperature, in the absence of disorder and commensurability effects such crystals have a perfect triangular lattice and a long-range order. They possess collective modes referred to as magnetophonons. Wigner crystal has a single magnetophonon branch [10], bubble phases may have several [11]; however, in both cases only one mode is gapless. The following discussion is devoted exclusively to the dynamics of the gapless mode. Quasiclassically, a magnetophonon excitation can be understood as a coherent precession of M-electron bubbles around their equilibrium positions, with the charge distribution (form-factor) of individual bubbles being fixed. In this picture the dynamical degrees of freedom are the centers of mass of the bubbles.

The effects of disorder on gapless magnetophonon excitations belong to a broad class of phenomena known as *pinning*. The pinning affects a variety of physical systems. It has been extensively studied in the context of conventional charge-density waves [12] and vortex lattices in superconductors [13]. Two pinning mechanisms are distinguished, the individual and the collective ones. In this paper we focus on the latter. The collective pinning is the regime where the random potential due to impurities and other defects is too weak to significantly deform the crystalline lattice, so that the crystal is well ordered at small length scales. However, the cumulative effect of the disorder eventually dominates the crystal elasticity at a pinning length, which is much larger than the lattice constant a. The long-range order of the crystal is thereby destroyed. Similarly, the low-frequency collective modes are unaffected by disorder at the scale of a, but get localized at some larger scale. These localized modes give rise to a maximum at a disorder-dependent frequency ω_p in the real part of diagonal conductivity $\Re\mathrm{e}\sigma(\omega)$. Such maxima (pinning modes) have been studied primarily in conventional charge-density wave materials [12,14]. However, a few observations of similar absorption lines due to 2DEG subject to a strong magnetic field have also been reported [15]. The aforementioned latest experiments on high-mobility 2DEG provided much more extensive and higher resolution data in the strong-field regime [4,5,6,7] and also detected pinning resonances in weak fields [8], which were interpreted as signatures of bubble phases and Wigner crystals at higher Landau levels. The quantities that can be extracted and analyzed most reliably are (i) the position ω_p of the peak in $\Re\mathrm{e}\,\sigma$, (ii) its width $\Delta\omega_p$, and (iii) the area F under the curve (see Fig. 1).

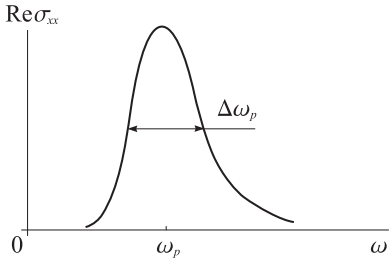

Fig. 1. The sketch of the absorption line due to pinning.

(i) The dependence of ω_p on magnetic field and disorder is often discussed in the framework of a popular physical picture [16,17] illustrated by Fig. 2. Each localized magnetophonon mode is visualized as precession (or drift) of a crystallite with linear dimension of the order of the pinning length R_c in a potential well created by disorder. Let $\omega_c = eB/m_e c$ be the cyclotron frequency in the external magnetic field B. For a potential well with curvature $\sim M_0\omega_0^2$, where M_0 is the total mass of the patch, an elementary calculation gives the frequency of the drift motion $\omega_p \sim \omega_0^2/\omega_c$ in the experimentally relevant case $\omega_c \gg \omega_p$. If ω_0 depends only on the amount of disorder (e.g., impurity concentration) but not on B, then $\omega_p \propto 1/B$.

(ii) As far as $\Delta\omega_p$ is concerned, in a random system of independent oscillators we expect a broad distribution of ω_0^2 [17], which implies a broad spectrum of their eigenfrequencies, i.e., $\Delta\omega_p \sim \omega_p$.

(iii) Finally, for the integrated oscillator strength F, this model predicts [16], $F = (\pi/2)(e^2 n_e/m_e)(\omega_p/\omega_c)$, where n_e and m_e are the electron concentration and effective mass, respectively.

Despite a certain appeal of these arguments, their predictions are not supported by experiments. First,

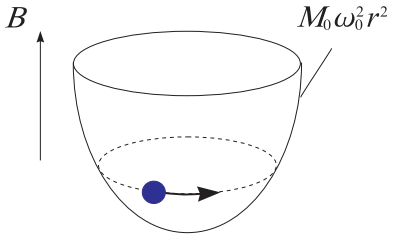

Fig. 2. Naive cartoon of a localized magnetophonon mode. The ball represents a single domain of the pinned crystal, which has mass M_0. The paraboloid symbolizes the pinning potential in which this domain resides. The dashed line shows the drift trajectory in the two-dimensional plane $\mathbf{r} = (x, y)$.

the pinning frequency shows a complicated nonmonotonic dependence on B. Second, the absorption line is very narrow. Quality factors $Q = \omega_p/\Delta\omega_p$ as large as ten were reported in the published literature on the high-field Wigner crystal [4,6,7] and lower but still respectable quality factors $Q \sim 3$ for the bubbles. Only the integrated oscillator strength F is in a rough agreement [8] with the simple theory.

It turns out that the anomalous B-dependence can in principle be explained by the interplay between the correlation length of the pinning potential and the B-dependent form-factor of the electron wavefunctions [18,19,9]. On the other hand, to explain the small linewidth one has to develop a theory that goes beyond the cartoon depicted in Fig. 2. Such a theory is the subject of this paper. We will show that the line narrowing is due to the long-range Coulomb interaction in the electron crystal.

2. Definition of the model and the pinning frequency

We treat Wigner and bubble phases on the same footing, as crystals of *classical* particles of mass Mm_e, charge Me, and average concentration, n_e/M. They interact with each other via potential $V(\mathbf{r})$ and are subject to a weak random potential $U(\mathbf{r})$. We assume that V and U incorporate the appropriate form-factors, calculated using the quantum wavefunctions of the bubbles [1,3]. (This is the only place where quantum mechanics enters our model.) We describe the deviation of the crystal lattice from the ideal periodicity in terms of the elastic displacement field $\mathbf{u}_{el} = \mathbf{u}^{(0)} + \mathbf{u}$, which we split into the static ground-state distortion $\mathbf{u}^{(0)}(\mathbf{r})$ and the magnetophonon fluctuations $\mathbf{u}(\mathbf{r}, t)$. We restrict ourselves to the harmonic approximation, where magnetophonon modes are obtained by diagonalizing the dynamical matrix $[\mathbf{D}]^{-1} = [\mathbf{D}^0]^{-1}\delta_{\mathbf{q}_1,\mathbf{q}_2} + \delta\tilde{\mathbf{S}}(\mathbf{q}_1 - \mathbf{q}_2)$, where $\mathbf{D}^0 = \mathbf{D}^0(\mathbf{q}, \omega)$ is a dynamical matrix of a uniformly pinned crystal. In the convenient basis of transverse (T) and longitudinal (L) components, $\mathbf{u}(\mathbf{q}) = \hat{\mathbf{q}}u_L(\mathbf{q}) + [\hat{\mathbf{z}} \times \hat{\mathbf{q}}]u_T(\mathbf{q})$, where $\hat{\mathbf{q}} = \mathbf{q}/|\mathbf{q}|$, $\mathbf{D}^0$ has the form [16,10]

$$[\mathbf{D}^0]^{-1} = \begin{bmatrix} \mu q^2 + S_0 - \rho\omega^2 & -i\rho\omega\omega_c \\ i\rho\omega\omega_c & \lambda q^2 + S_0 - \rho\omega^2 \end{bmatrix}, \quad (1)$$

where $\rho = m_e n_e$ is the average mass density, $\mu \sim M^2e^2/\kappa a^3$ is the shear elastic modulus, $\lambda = \lambda(q) = 2\pi e^2 n_e^2/\kappa q$ is the effective bulk modulus, and κ is the dielectic constant of the medium. The q-dispersion of λ is due to long-range Coulomb interaction. At small q, we have $\lambda(q) \gg \mu$, i.e., compressions cost much more energy than shear deformations. Parameter S_0 is the average value of the diagonal components of the curvature tensor $\mathbf{S} = \nabla\nabla U(\mathbf{r})$ evaluated at the ground-state particle positions. From standard collective pinning arguments, we expect $S_0 \sim \mu/R_c^2 \equiv \rho\omega_0^2$, where R_c is the pinning length related to the amplitude of the random potential U and the shear modulus μ [9]. The quantity $\delta\tilde{\mathbf{S}} \equiv \tilde{\mathbf{S}} - S_0\mathbf{I}$ describes fluctuations of the curvature, where $\mathbf{I}$ is the identity matrix and tilde denotes the Fourier transform. Our goal is to calculate the ac conductivity, $\sigma(\omega) = -ie^2n_e^2\omega\langle\mathbf{D}(\omega + i0)\rangle$, where $\langle\ldots\rangle$ denotes disorder averaging. The conductivity can be expressed in terms of the self-energy $\Pi(\mathbf{q}, \omega) \equiv S_0\mathbf{I} + \left(\langle\mathbf{D}\rangle^{-1} - [\mathbf{D}^0]^{-1}\right)$, as follows:

$$\Re\mathrm{e}\,\sigma(\omega) = e^2n_e^2\omega\,\Im\mathrm{m}\,\frac{\Pi(0,\epsilon) - \epsilon}{[\Pi(0,\epsilon) - \epsilon]^2 - \epsilon\epsilon_c}. \quad (2)$$

Here we introduced convenient "energy" variables $\epsilon \equiv \rho\omega^2$ and $\epsilon_c \equiv \rho\omega_c^2$. From Eq. (2) one can see that in strong magnetic fields the conductivity as a function of ω has a maximum of width $\Delta\omega_p = -\Im\mathrm{m}\,\Pi(0, \rho\omega_p^2)/\rho\omega_c$ centered at $\omega_p = \Re\mathrm{e}\,\Pi/\rho\omega_c$. Up to logarithmic factors [9], $\Re\mathrm{e}\,\Pi \sim S_0$, and so $\omega_p = \omega_0^2/\omega_c$. Thus, the position of the conductivity peak is simply related to the pinning length R_c, in basic agreement with the arguments given in Sec. 1 (and as mentioned above, R_c can be straighforwardly expressed in terms of the microscopic parameters of the model). The lineshape and

linewidth require much more elaborate analysis given in the next section.

3. Lineshape and linewidth of the pinning mode

To find Π and σ we have to resort to certain approximations, which we motivate by physical arguments. As a starting point, consider a simpler model of a pinned one-dimensional (1D) electron crystal with short-range (screened) interaction V in the absence of any magnetic field. It has been known from early work [20,21] that $\Re\mathrm{e}\,\sigma(\omega)$ has a broad maximum at the characteristic pinning frequency $\omega_p^{1D} = v/R_c$, where R_c is the pinning length and v is the sound velocity. However, there has been a disagreement about the behavior of σ at small ω. Recently, the present author [22] and later also Gurarie and Chalker [23] advanced analytical and numerical arguments that $\Re\mathrm{e}\,\sigma(\omega) \propto \omega^4$ for $\omega \ll \omega_p^{1D}$. The physical picture is as follows [22]. In 1D, elastic displacement u is a scalar and there is a formal analogy between the phonon problem and 1D localization in a random potential $S(x) = U''(x)$. Indeed, the phonon mode with "energy" ϵ_i must satisfy the Schrödinger equation $-\rho v^2 u_i'' + S(x)u_i(x) = \epsilon_i u$. Borrowing standard arguments from the 1D localization literature, one can show that phonon eigenmodes with $\omega \lesssim \omega_p^{1D}$ have localization length $\sim R_c$. Each mode can be viewed as harmonic oscillations of a segment of length R_c in a potential well created by the pinning centers. This echoes the picture depicted in Fig. 2 and arguments given in Sec. 1. The ω^4-law for the the low-frequency ("soft") modes follows from a careful derivation of the the statistical distribution of the curvatures of such collective potential wells. One finds [22] that the density of states $\nu = \langle\delta(\epsilon-\epsilon_i)\rangle$ of the eigenmodes goes as $\nu(\epsilon) \propto \epsilon^s$ with $s = 3/2$. The conductivity is proportional to ν, and once the Jacobian of the transformation from ϵ to ω is taken into account, one obtains $\Re\mathrm{e}\,\sigma \propto \omega^{2s+1} = \omega^4$. What is important here is that the derivation of ν and the exponent s is rather insensitive to microscopic details. Therefore, ω^4-law is expected to hold in higher dimensions and for other types of pinning models [24,23]. Shortly below, we will make use of this universality.

Let us now return to the 2D case but first examine a model, which is a truncated version of the original one. Consider what happens if we remove by hand all elements of the dynamical matrix $\mathbf{D}$ that connect L and T modes. (On some crude level, it corresponds to a 2D crystal in zero magnetic field.) As in 1D case, we reduce the problem to solving a Schrödinger equation. Now we have two such equations,

$$\mathbf{H}_T u_T \equiv -\mu\nabla^2 u_T + S_T(\mathbf{r})u_T = \epsilon u_T \qquad (3)$$

for T-modes and $-\lambda\nabla^2 u_L + S_L(\mathbf{r})u_L = \epsilon u_L$ for L-modes. Here S_T and S_L are the T-T and L-L components of the matrix $\mathbf{S}$, and λ should be inderstood as integral operator. What is the structure of the resultant eigenmodes? The T-modes with $\omega < \omega_0$ again form a set of oscillators localized on the scale of the pinning length R_c (ω_0, introduced in Sec. 2, can be thought of as the $B = 0$ pinning frequency). The soft T-modes correspond to $\omega \ll \omega_0$, i.e., $\epsilon \ll \rho\omega_0^2 \equiv \Pi_0$. Turning to the L-modes, in principle, we also obtain a set of local oscillators. If λ could be replaced by some q-independent constant much larger than μ, as in the case of Coulomb interaction screened by a nearby metallic gate, then the localization length of L-modes would be $R_L = R_c\sqrt{\lambda/\mu}$. It is much larger than R_c because S_L has about the same rms fluctuations as S_T yet the L-modes are much stiffer and resist localization effects more efficiently. If q-dispersion of λ is taken into account, then one finds [9] that the eventual localization does occur, but at a scale so large that it can be treated as infinite for all practical purposes. In this approximation, randomness in S_L does not affect the dynamics, so that S_L can be replaced by S_0. We arrived at a system of localized T-phonons and delocalized L-phonons. In such a system, $\Re\mathrm{e}\,\sigma$ has an infinitely sharp pinning mode.

Let us now reinstate the L-T mixing. We will show that localization does occur at some reasonable scale R_M in this case and that $\Delta\omega_p$ is finite albeit much smaller than ω_p. However, this is not a trivial task because the dynamical equations become much more complicated. Fortunately, in the large-B limit there are two simplifications. First, we only need to consider mixing due to the Lorentz force. (The L-T mixing due to disorder is not important for the main results.) Second, the inertial terms $-\rho\omega^2$ in $\mathbf{D}^0$ [Eq. (1)] can be neglected. The equation for u_L becomes

$$(-\lambda\nabla^2 + S_0)u_L = \epsilon\epsilon_c[\mathbf{H}_T]^{-1}u_L. \qquad (4)$$

The resolvent of the operator $\mathbf{H}_T$ [Eq. (3)] on the right-hand side of Eq. (4) can be written in terms of local-

ized T eigenmodes discussed above. We will see that $R_M \gg R_c$; therefore, it is legitimate to coarse-grain the model on the scale R_c, so that each localized oscillator becomes represented by a single site. This leads to the equation

$$(-\lambda\nabla^2 + \epsilon_0)u_L = \sum_j (\epsilon\epsilon_c/\epsilon_j)R_c^2\delta(\mathbf{r}-\mathbf{R}_j)u_L. \quad (5)$$

In the real space, it reads

$$u_L(\mathbf{r}) = \epsilon\epsilon_c \sum_j \frac{u_L(\mathbf{R}_j)}{\epsilon_j} K(\mathbf{r}-\mathbf{R}_j), \quad (6)$$

where $K(r)$ is the inverse Fourier transform of $R_c^2/[\lambda(q)q^2+\epsilon_0]$. Function K is of the order of $K_0 = R_c^2/\lambda$ at $r \sim R_c$. At large r, it decays as $1/r^3$.

The spectrum of eigenmodes can be obtained from Eq. (6) by setting $\mathbf{r} = \mathbf{R}_j$ and solving the resultant system of linear equations. For example, if we neglect randomness and replace ϵ_j's by their typical value Π_0, we obtain $\epsilon \sim \Pi_0/\epsilon_c$, and so $\omega_p \sim \omega_0^2/\omega_c$ in agreement with Sec. 2.

Let us now try to account for the randomness. Consider a mode with $\omega \sim \omega_p$. It is easy to see that soft modes with energies $\epsilon_j \ll \epsilon_s = (\mu/\lambda)\Pi_0$ have a dramatic effect on u_L. Within a distance $\sim (\lambda/\mu)R_c$ to the locations of such a mode, u_L is strongly suppressed. We interpret this as an indication that these soft modes act as strong scatterers for the magnetophonons and propose that the magnetophonon localization length is of the order of the average distance between these scatterers, $R_M \sim [\epsilon_s \nu(\epsilon_s)]^{-1/2}$ (see Fig. 3). Using the 3/2-law for the soft mode density of states $\nu(\epsilon)$, we obtain $R_M \sim (\lambda/\mu)^{5/4}R_c$. Here and in previous formulas $\lambda = \lambda(1/R_c)$.

Let us now evaluate $\Delta\omega_p$. To the left-hand side of Eq. (4) each scatterer contributes a term of the order of $(\lambda/R_c^2)(R_c/R_M)^2$, where the first factor is the characteristic value of $\lambda\nabla^2$ in the vicinity of the scatterer and the second term is the ratio of the area $\sim R_c^2$ where the nonuniformity in u_L is concentrated to the total localization area R_M^2. The net effect of this term is to shift ϵ by a random amount of the order of $\Delta\epsilon \sim (\lambda/\epsilon_c)(R_c/R_M)^2$. Such shifts produce an inhomogeneously broadened pinning mode with the quality factor $Q = \omega_p/\Delta\omega_p \sim \epsilon/\Delta\epsilon \sim (\lambda/\mu)^{3/2} \gg 1$. This result was previously obtained by a somewhat different method in Ref. [22] where the lineshape was also calculated:

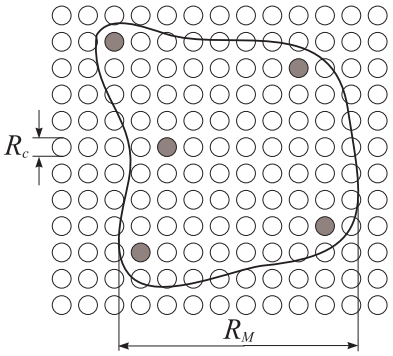

Fig. 3. Schematic structure of the localized magnetophonon eigenstate. Circles represent the T-modes. Soft modes that act as strong scatterers are shaded.

$$\sigma(\omega) = -i\frac{e^2 n_e \omega}{m_e\omega_0^2}\frac{1-i(\omega/\Omega)^{3/2}}{[1-i(\omega/\Omega)^{3/2}]^2-(\omega/\omega_p)^2}. \quad (7)$$

Here $\Omega = \omega_p\sqrt{\lambda/\mu}$. It should be mentioned that other theories [18,19] give different predictions for $\Delta\omega_p$. Their critique is given in Ref. [9].

4. Comparison with experiments and conclusions

The main uncertainty in comparing the outlined theory with the experiment is the nature of disorder. It is far from obvious, e.g., why pinning centers should be weak rather than strong [25] in GaAs-based 2DEG. However, assuming this is the case, we can take empirical values of ω_p and n_e and work back to the disorder parameters to see if they are reasonable. In this manner, one obtains $R_c \sim 6a$ in samples with largest Q [9,7]. For the root-mean square amplitude of the random potential we get $U \sim 0.2$ K. As remarked in Sec. 1, the pinning frequency can also give information about the correlation length ξ of the random potential. It is easy to show [18,19,9] that ω_p as a function of B should reach a maximum at the point where ξ is of the order of the size of the bubbles (a few magnetic lengths). Using this approach, ξ of the order of a few nm can be estimated. Fertig [19] suggested that the disorder with such characteristics may originate from surface roughness.

Regarding the linewidth, our theory predicts quality factors $Q \sim 200$ in the limit of infinite sample size and zero temperature. Finite width of the transmission

line ($\sim 30\,\mu$m or $10^3 a$) in the experiments imposes the upper limit of about 30 on achievable Q. The remaining discrepancy may be related to quantum and thermal effects, which warrant further study.

Acknowledgements

I thank David Huse for previous collaboration on the topics reported here and Yong Chen, Lloyd Engel, Rupert Lewis, and Dan Tsui for valuable discussions of the experiments. This work is supported by Hellman Scholarship Award at University California San Diego.

References

[1] M. Shayegan, Ch. 9 in Perspectives in Quantum Hall Effect, edited by S. Das Sarma and A. Pinczuk, Wiley, New York, 1997; H. A. Fertig, *ibid.*, Ch. 3.

[2] For review, see J. P. Eisenstein, M. P. Lilly, K. B. Cooper, L. N. Pfeiffer, and K. W. West, Physica E **9** (2001) 1; J. P. Eisenstein, Solid State Commun. **117** (2001) 132.

[3] For review, see M. M. Fogler, pp. 98-138 in High Magnetic Fields: Applications in Condensed Matter Physics and Spectroscopy, Springer-Verlag, Berlin, 2002; cond-mat/0111001. For original work, see A. A. Koulakov, M. M. Fogler, and B. I. Shklovskii, Phys. Rev. Lett. **76** (1996) 499; M. M. Fogler, A. A. Koulakov, and B. I. Shklovskii, Phys. Rev. B **54** (1996) 1853; M. M. Fogler and A. A. Koulakov, Phys. Rev. B **55** (1997) 9326.

[4] C.-C. Li, L. W. Engel, D. Shahar, D. C. Tsui, and M. Shayegan, Phys. Rev. Lett. **79** (1997) 1353.

[5] P. F. Hennigan, A. Beya, C. J. Mellor, R. Gaal, F. I. B. Williams, and M. Henini, Physica B **249-251** (1998) 53; A. S. Beya, Ph.D. thesis, L'Université Paris VI (1998).

[6] C.-C. Li, J. Yoon, L. W. Engel, D. Shahar, D. C. Tsui, and M. Shayegan, Phys. Rev. B **61** (2000) 10905.

[7] P. D. Ye, L. W. Engel, D. C. Tsui, R. M. Lewis, L. N. Pfeiffer, and K. W. West, Phys. Rev. Lett. **89** (2002) 176802.

[8] R. M. Lewis, P. D. Ye, L. W. Engel, D. C. Tsui, L. N. Pfeiffer, and K. W. West, Phys. Rev. Lett. **89** (2002) 136804.

[9] M. M. Fogler and D. A. Huse, Phys. Rev. B **62** (2000) 7553.

[10] L. Bonsall and A. A. Maradudin, Phys. Rev. B **15** (1977) 1959. See also R. Côté and A. H. MacDonald, Phys. Rev. B **44** (1991) 8759.

[11] R. Côté, C. Doiron, J. Bourassa, and H. A. Fertig, cond-mat/0304412.

[12] G. Grüner, Rev. Mod. Phys. **60** (1988) 1129.

[13] G. Blatter, M. V. Feigel'man, V. B. Geshkenbein, A. I. Larkin, and V. M. Vinokur, Rev. Mod. Phys. **66** (1994) 1125.

[14] P. Brüesch, S. Strässler, and H. R. Zeller, Phys. Rev. B **12** (1975) 219; L. Degiorgi and G. Grüner, Phys. Rev. B **44** (1991) 7820.

[15] M. A. Palaanen, R. L. Willett, P. B. Littlewood, R. R. Ruel, K. W. West, L. N. Pfeiffer, and D. J. Bishop, Phys. Rev. B **45** (1992) 11342.

[16] H. Fukuyama and P. A. Lee, Phys. Rev. B **18** (1978) 6245.

[17] B. G. A. Normand, P. B. Littlewood, and A. J. Millis, Phys. Rev. B **46** (1992) 3920.

[18] R. Chitra, T. Giamarchi, and P. Le Doussal, Phys. Rev. Lett. **80** (1998) 3827.

[19] H. A. Fertig, Phys. Rev. B **59** (1999) 2120.

[20] V. M. Vinokur, M. B. Mineev, and M. V. Feigel'man, Zh. Eksp. Teor. Fiz. **81** (1980) 2142. [Sov. Phys. JETP **54** (1981) 1138].

[21] T. Giamarchi and H. J. Schulz, Phys. Rev. B **37** (1988) 325 and references therein.

[22] M. M. Fogler, Phys. Rev. Lett. **88** (2002) 186402.

[23] V. Gurarie and J. T. Chalker, Phys. Rev. Lett. **89** (2002) 136801.

[24] I. L. Aleiner and I. M. Ruzin, Phys. Rev. Lett. **72** (1993) 1056.

[25] I. M. Ruzin, S. Marianer, and B. I. Shklovskii, Phys. Rev. B **46** (1992) 3999.